Submitted 24 September 2001; Accepted 4 December 2001 – To appear in the March, 2001 AJ
Preprint typeset using LaTeX style emulateapj v. 14/09/00

THE KPNO INTERNATIONAL SPECTROSCOPIC SURVEY. III. [O III]-SELECTED SURVEY LIST.

John J. Salzer[1], Caryl Gronwall[1,2], and Vicki L. Sarajedini[3]
Astronomy Department, Wesleyan University, Middletown, CT 06459; slaz@astro.wesleyan.edu
Valentin A. Lipovetsky[1,4] and Alexei Kniazev[1,5]
Special Astrophysical Observatory, Russian Academy of Sciences, Nizhny Arkhyz, Karachai-Circessia 357147, Russia
J. Ward Moody
Department of Physics & Astronomy, Brigham Young University, Provo, UT 84602; jmoody@astro.byu.edu
Todd A. Boroson
National Optical Astronomy Obs., P.O. Box 26732, Tucson, AZ 85726; tyb@noao.edu
Trinh X. Thuan
Astronomy Department, University of Virginia, Charlottesville, VA 22903; txt@starburst.astro.virginia.edu
Yuri I. Izotov
Main Astronomical Observatory, National Academy of Sciences of Ukraine, Goloseevo, Kiev 03680, Ukraine; izotov@mao.kiev.ua
José L. Herrero
BBN Technologies, Cambridge, MA 02140; jose@world.std.com
Lisa M. Frattare[1]
Space Telescope Science Institute, Baltimore, MD 21218; frattare@stsci.edu
Submitted 24 September 2001; Accepted 4 December 2001 – To appear in the March, 2001 AJ

ABSTRACT

The KPNO International Spectroscopic Survey (KISS) is an objective-prism survey for extragalactic emission-line objects. It combines many of the features of previous slitless spectroscopic surveys with the advantages of modern CCD detectors, and is the first purely digital objective-prism survey for emission-line galaxies. Here we present the first list of emission-line galaxy candidates selected from our blue spectral data, which cover the wavelength range 4800 − 5500 Å. In most cases, the detected emission line is [O III]λ5007. The current survey list covers a one-degree-wide strip located at $\delta = 29° \ 30'$ (B1950.0) and spanning the right ascension range $8^h \ 30^m$ to $17^h \ 0^m$. An area of 116.6 deg^2 is covered. A total of 223 candidate emission-line objects have been selected for inclusion in the survey list (1.91 deg^{-2}). We tabulate accurate coordinates and photometry for each source, as well as estimates of the redshift, emission-line flux, and equivalent width based on measurements of the digital objective-prism spectra. The median apparent magnitude of the sample is B = 18.2, and galaxies with redshifts approaching z = 0.1 are detected. The properties of the KISS emission-line galaxies are examined using the available observational data, and compared to previous surveys carried out with photographic plates as well as with the Hα-selected portion of KISS.

Subject headings: galaxies: emission lines — galaxies: Seyfert — galaxies: starburst — surveys

1. INTRODUCTION

The KPNO International Spectroscopic Survey (KISS) is an ongoing objective-prism survey which targets the detection of large numbers of extragalactic emission-line sources. KISS attempts to build upon previous, extremely fruitful surveys for these types of objects, which have been responsible for the cataloging of a large proportion of the known starburst galaxies, Seyfert galaxies, and QSOs. Our survey method is similar to many of these previous surveys, which have been carried out with Schmidt telescopes and photographic plates (e.g., Markarian 1967, Smith *et al.* 1976, MacAlpine *et al.* 1977, Pesch & Sanduleak 1983, Wasilewski 1983, Markarian *et al.* 1983, Zamorano *et al.* 1994, Popescu *et al.* 1996, Surace & Comte 1998, Lipovetsky *et al.* 1998). The fundamental difference between KISS and these previous surveys is that we utilize a CCD as our detector. There are several obvious advantages of CCDs over photographic plates for this type of survey, including much higher quantum efficiency, lower noise, good spectral response over the entire optical portion of the spectrum, and large dynamic range. In addition, CCDs enable us to use automated selection methods to detect emission-line galaxies (ELGs), and allow us to quantify the selection function and completeness limit directly from the survey data. With the advent of large format CCDs in the past decade, the large areal coverage provided by the wide-field imaging capability of Schmidt telescopes makes digital surveys like KISS possible. The combination of increased depth and large areal coverage leads to substantial im-

[1] Visiting Astronomer, Kitt Peak National Observatory. KPNO is operated by AURA, Inc. under contract to the National Science Foundation.
[2] present address: Department of Physics & Astronomy, Johns Hopkins University, Baltimore, MD 21218; caryl@adcam.pha.jhu.edu.
[3] present address: Department of Astronomy, University of Florida, Gainesville, FL 32611; vicki@astro.ufl.edu.
[4] Deceased 22 September 1996.
[5] present address: Max Planck Institut für Astronomie, Königstuhl 17, D-69117, Heidelberg, Germany; kniazev@mpia.de.

provements compared to the previous photographic surveys listed above.

The primary goal of KISS is to produce a high-quality survey whose selection function and completeness limits can be accurately quantified so that the resulting catalog of ELGs will be useful for a broad range of studies requiring statistically complete galaxy samples. We also want to reach substantially deeper than previous objective-prism surveys.

A complete description of the survey method employed for KISS is given in the first paper in this series (Salzer *et al.* 2000, hereafter Paper I). KISS is a *line-selected* survey, meaning that the objective-prism spectra are searched for the presence of an emission feature. As described in Paper I, the first survey strip was observed in two distinct spectral regions. One covered the blue portion of the optical spectrum (4800 – 5500 Å), while the second covered the wavelength range 6400 – 7200 Å in the red part of the spectrum. The first red survey list is given in Salzer *et al.* (2001, hereafter KR1). The current paper presents the initial KISS list of [O III]-selected ELG candidates. The format of the current paper follows closely that of KR1. In addition to listing the ELGs, we provide substantial observational data for each object. This includes accurate photometry and astrometry for each source, as well as estimates of each galaxy's redshift, line flux, and equivalent width. These data are used to examine the properties of the KISS ELGs in Section 4.

2. OBSERVATIONS

All survey data were acquired using the 0.61-meter Burrell Schmidt telescope[6]. The detector used for all data reported here was a 2048 × 2048 pixel STIS CCD (S2KA). This CCD has 21-μm pixels, which yields an image scale of 2.03 arcsec/pixel. The overall field-of-view is 69 × 69 arcmin, and each image covers 1.32 square degrees. Due to the coarse pixel scale, seeing variations do not adversely affect the survey data. Nearly all of the direct and spectral images used to construct the survey are undersampled (i.e., have point-spread-function widths of less than two pixels). The blue survey spectral data were obtained with a 2° prism, which provided a reciprocal dispersion of 19 Å/pixel at 5000 Å. The spectral data were obtained through a special filter designed for the survey, which covered the spectral range 4800 – 5500 Å (see Figure 1 of Paper I for the filter transmission curve).

The survey data consist of the spectral images, obtained with the objective prism on the telescope, plus direct images taken without the prism through standard B and V filters. Full details are presented in Paper I. The primary emission line detected in the blue spectral data is [O III]λ5007. It is possible that the Hβ line could be stronger than [O III]λ5007 and hence be the feature seen in the survey spectra. However, ELGs with Hβ stronger than [O III] tend to be fairly luminous starburst galaxies with low equivalent width lines. Such objects tend to be missed in line-selected objective-prism surveys like KISS, unless the survey is carried out in the red and selects via Hα. Hence, we expect that the large majority of ELGs found in the current survey are detected via their [O III] emission. Follow-up spectra for 123 blue-selected KISS ELGs confirm this (see section 4). The redshift range over which we are able to detect ELGs, which is limited by the spectral filter described above, is z = 0 to 0.09 for the [O III] line, and z = 0 to 0.13 for Hβ. Finally, we mention the possibility that higher redshift galaxies (z = 0.29 to 0.47) might be detected via [O II]λ3727 emission. These objects would need to be quite luminous and possess fairly strong emission lines in order to be detectable. To date no such high redshift objects have been found in our limited follow-up spectra (although some have been found in the red survey – see KR1).

This blue survey consists of a contiguous strip of fields observed at a constant declination ($\delta = 29° \; 30'$ (B1950.0)). The right ascension range covered is $8^h \; 30^m$ to $17^h \; 0^m$ (B1950.0). This area was chosen to overlap completely the Century Redshift Survey (Geller *et al.* 1997; Wegner *et al.* 2001). Table 1 lists information about the observing runs during which the survey observations were obtained. The first column gives the UT dates of the run, while the second column indicates the number of nights on which observations were obtained. At least some data were obtained on 40 of 53 scheduled nights (75%). The last two columns indicate the number of direct and spectral images, respectively, obtained during each run. It was common practice to obtain both direct and objective-prism images during each run, with the prism being on the telescope for about half of each block of time. Note that the values listed in columns 3 and 4 represent the number of images actually used for the survey. Due to imperfect observing conditions, many images taken during the earlier runs were repeated later in order to replace lower quality images with better ones. The most common problems plaguing the early data were poor telescope focus and wind shaking of the telescope which resulted in extended images. The bulk of the data used to construct the survey were obtained in 1996 and 1997.

A goal of the survey was to obtain data that were of uniform depth and image quality for all survey fields. To that end, we employed a fixed exposure time for all survey observations. Direct images had exposure times of 300 s in V and 600 s in B (although observations taken during the first few runs were slightly longer). All spectral data consist of four 720 s exposures of each field, for a total exposure time of 48 minutes per field. The telescope was dithered by ∼10 arcsec between exposures in order to move sources off of bad columns on the CCD. Data processing procedures are detailed in Paper I. The analysis of the survey data was carried out using an IRAF[7]-based software package written by members of the KISS team. This package is described in Herrero *et al.* (2002).

3. FIRST BLUE LIST OF THE KPNO INTERNATIONAL SPECTROSCOPIC SURVEY

3.1. *Selection Criteria*

[6] Observations made with the Burrell Schmidt of the Warner and Swasey Observatory, Case Western Reserve University. During the period of time covered by the observations described here, the Burrell Schmidt was operated jointly by CWRU and KPNO.

[7] IRAF is distributed by the National Optical Astronomy Observatories, which are operated by AURA, Inc. under cooperative agreement with the National Science Foundation.

The selection of ELG candidates from the objective-prism images is described in detail in KR1. Here we provide a brief summary of the key issues. The selection methods used for the current (blue) spectral data are identical to those used for the red data in KR1.

The KISS reduction software selects ELG candidates by searching the extracted objective-prism spectra for objects with 5σ emission features. This is the primary selection criterion of the survey. After this automated selection process, the candidate ELGs are checked manually and many spurious sources are rejected. These rejected sources often consist of very faint objects with noisy spectra, and brighter sources with strong spectral breaks within the KISS bandpass. Following the evaluation of the software-selected candidates, the spectral images are scanned visually as a final check for possible 5σ sources that were missed by the software. These are typically objects with lines very close to the red end of the spectra, or bright galaxies with lower equivalent width lines where the continuum fitting process overestimates the continuum level slightly and hence underestimates the line strength. These objects are added to the KISS tables manually. For the current survey list, 17.8% of the objects were added to the final catalog during this visual search. The combination of the automatic software and this visual checking ensures that the sample is quite complete for objects with $\geq 5\sigma$ lines.

As mentioned in KR1, objects with emission lines between 4σ and 5σ are also flagged in the database tables and retained as possible ELGs. This sample of $<5\sigma$ sources is not statistically complete, and hence is not included in the main survey lists. Rather, we include these additional lower probability sources in a secondary list of ELG candidates which should be thought of as a supplement to the main KISS catalog.

3.2. *The Survey*

The list of ELG candidates selected in the blue survey is presented in Table 2. Because the survey data includes both photometrically-calibrated direct images and spectral images, we are able to include a great deal of useful information about each source, such as accurate photometry and astrometry and estimates of the redshift, emission-line flux, and equivalent width. Only the first page of the table is printed here; the complete table is available in the electronic version of the paper.

The contents of the survey table are as follows. Column 1 gives a running number for each object in the survey with the designation KISSB XXXX, where KISSB stands for "KISS blue" survey. This is to distinguish it from the red KISS survey (KR1). Columns 2 and 3 give the object identification from the KISS database tables, where the first number indicates the survey field (FXXXX), and the second number is the ID number within the table for that galaxy. This identifier is necessary for locating the KISS ELGs within the survey database tables. Columns 4 and 5 list the right ascension and declination of each object (J2000). The formal uncertainties in the coordinates are 0.25 arcsec in right ascension and 0.20 arcsec in declination. Column 6 gives the B magnitude, while column 7 lists the B−V color. For brighter objects the magnitude estimates have uncertainties of typically 0.05 magnitude, increasing to ∼0.10 magnitude at B = 20. Paper I includes a complete discussion of the precision of both the astrometry and photometry of the KISS objects. An estimate of the redshift of each galaxy, based on its objective-prism spectrum, is given in column 8. This estimate assumes that the emission line seen in the objective-prism spectrum is [O III]. Follow-up spectra for 123 ELG candidates from the current list show that this assumption is correct in the vast majority of cases. The formal uncertainty in these redshift estimates is $\sigma_z = 0.0049$ (see Section 4.1.3). There are three objects in the table with negative redshifts listed. In all three cases the measured value is just slightly negative (i.e., within the error quoted above), and two of the three have redshifts measured from follow-up spectra that are both small but positive. Columns 9 and 10 list the emission-line flux (in units of 10^{-16} erg/s/cm^2) and equivalent width (in Å) measured from the objective-prism spectra. The calibration of the fluxes is discussed in Section 4.1.2. These quantities should be taken as being representative estimates only. A simple estimate of the reliability of each source, the quality flag (QFLAG), is given in column 11. This quantity, assigned during the line measurement step of the data processing, is given the value of 1 for high quality sources, 2 for lower quality but still reliable objects, and 3 for somewhat less reliable sources. Column 12 lists the KISSR number from KR1 for objects that were selected in both the red and blue surveys. The red survey overlaps the blue for field numbers F1215 and above (excluding fields F1430, F1435, and F1440). There are 125 KISSB ELGs in the overlap area, and 113 (90%) of these are also cataloged in either KISSR or KISSRx (see KR1). Column 13 gives alternate identifications for KISS ELGs which have been cataloged previously. This is not an exhaustive cross-referencing, but focuses on previous objective-prism surveys which overlap part or all of the current survey area: Markarian (1967), Case (Pesch & Sanduleak 1983), Wasilewski (1983), and UCM (Zamorano *et al.* 1994). Also included are objects in common with the *Uppsala General Catalogue of Galaxies* (UGC, Nilson 1973).

A total of 223 ELG candidates are included in this first list of [O III]-selected KISS galaxies. The total area covered by the survey is 116.6 deg^2, meaning that there are 1.91 KISS ELGs per deg^2. This compares to the surface density of 0.1 galaxies per deg^2 from the Markarian survey, and 0.52 per deg^2 for the UM survey (MacAlpine *et al.* 1977), one of the deepest of the photographic surveys that selected exclusively by line emission (and primarily by [O III]). Of the total, 119 were assigned quality values of QFLAG = 1 (53.4%), 89 have QFLAG = 2 (39.9%), and 15 have QFLAG = 3 (6.7%). Based on our follow-up spectra to date, 99% (71 of 72) of the sources with QFLAG = 1 are *bona fide* emission-line galaxies, compared to 95% (42 of 44) with QFLAG = 2 and 86% (6 of 7) with QFLAG = 3. In total, 97% of KISSB ELG candidates with follow-up spectra are *bona fide* emission-line galaxies. The properties of the KISS galaxy sample are described in the next section.

Figure 1 shows an example of the finder charts for the KISS ELGs. These are generated from the direct images obtained as part of the survey. Figure 2 displays the extracted spectra derived from the objective-prism images

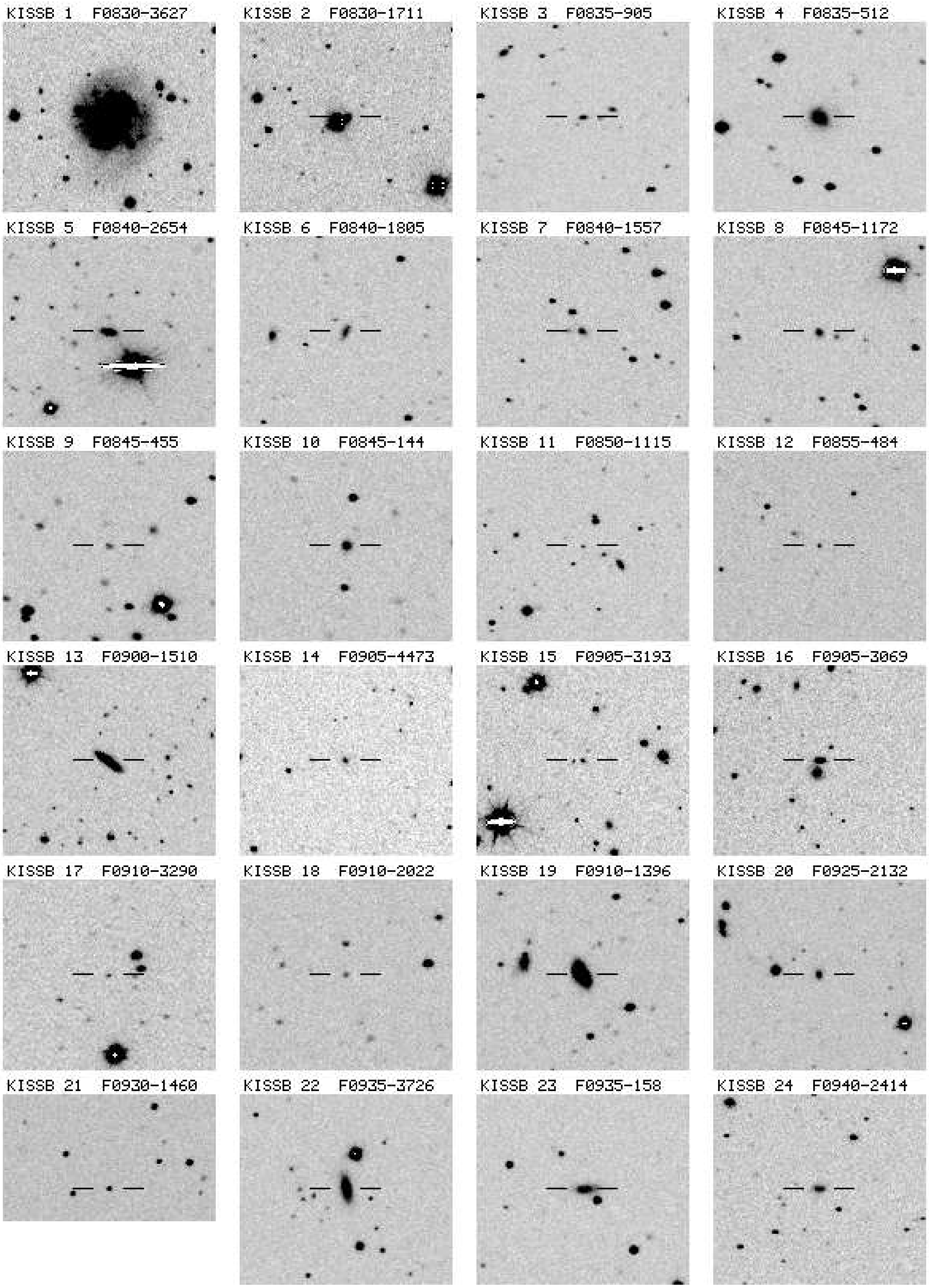

Fig. 1.— Example of finder charts for the KISS ELG candidates. Each image is 4.5 × 4.0 arcmin, with N up, E left. These finders are generated from the direct images obtained as part of the survey. In all cases the ELG candidate is located in the center of the image section displayed, and is indicated by the tick marks.

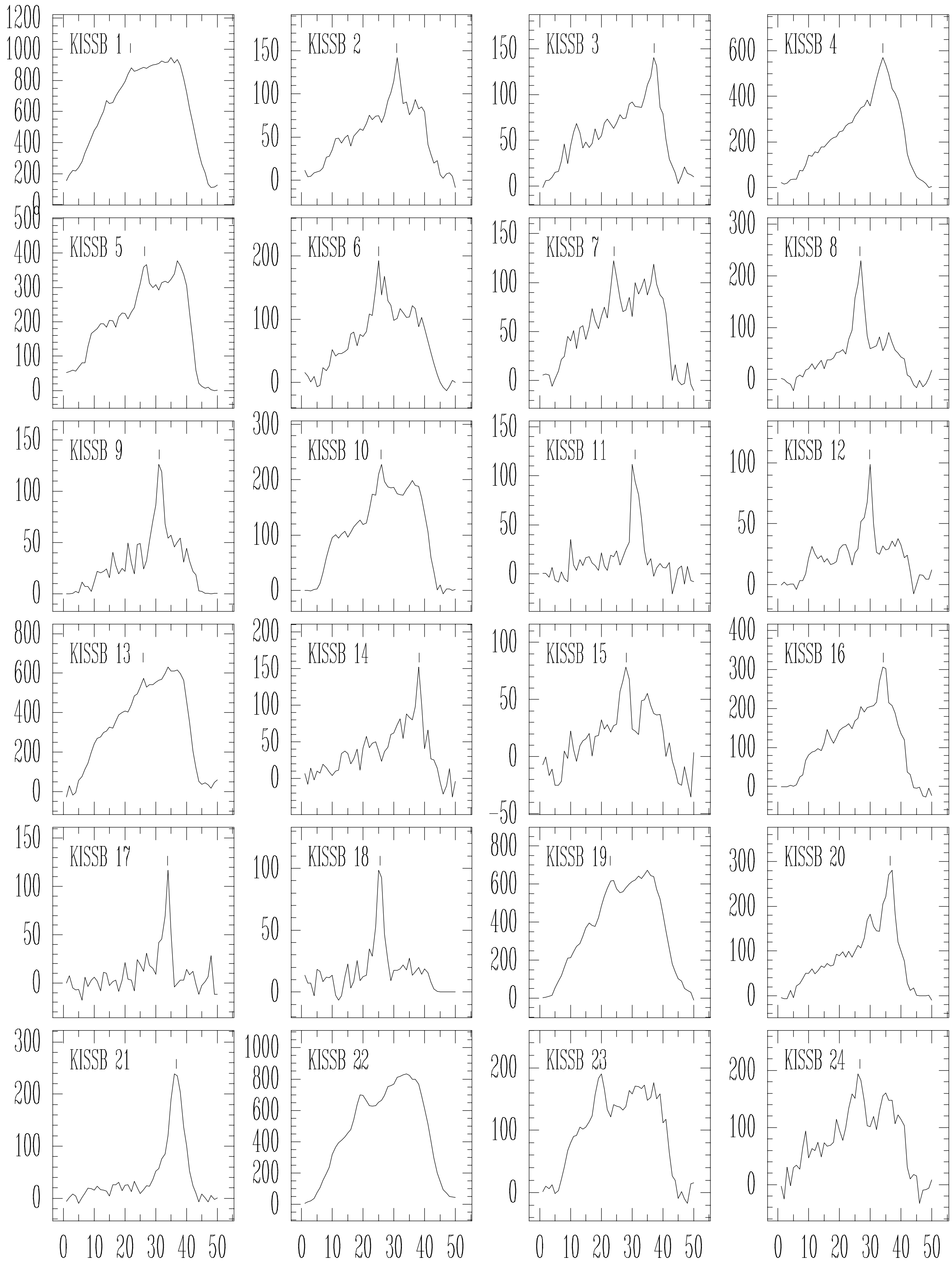

Fig. 2.— Plots of the objective-prism spectra for the first 24 KISS ELG candidates listed in Table 1. The spectral information displayed represents the extracted spectra present in the KISS database tables. The location of the putative emission line is indicated.

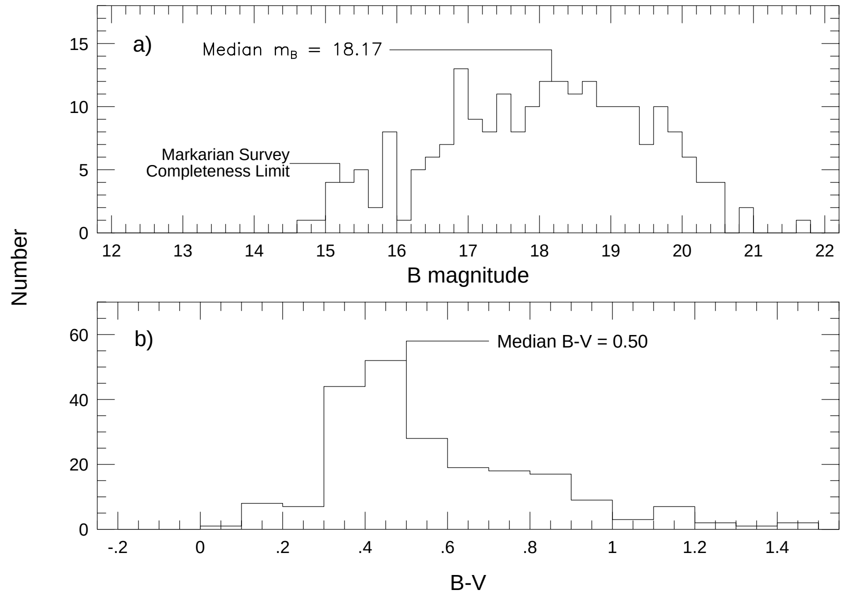

FIG. 3.— (a) Distribution of B-band apparent magnitudes for the 223 ELG candidates in the first [O III]-selected KISS survey list. The median brightness in the KISS sample is B = 18.17, with 8% of the galaxies having B > 20. Also plotted, for comparison, is the completeness limit of the Markarian survey. (b) Histogram of the B−V colors for the 223 ELG candidates. The median color of 0.50 is indicated.

for the first 24 ELGs in Table 1. Finder charts and spectral plots for all 223 objects in the KISS survey are available in the electronic version of this paper.

A supplementary table containing an additional 91 ELG candidates is included in the appendix of this paper (Table 3). These galaxies are considered to be lower probability candidates, having emission lines with strengths between 4σ and 5σ. These additional galaxies do not constitute a statistically complete sample, and should therefore be used with caution. However, there are likely many interesting objects contained in this supplementary list. Hence, following the precedent established in KR1, we list them in a separate table in order to give a full accounting of the ELGs in the fields surveyed.

4. PROPERTIES OF THE KISS ELGS

4.1. *Observed Properties*

One of the advantages of the KISS observing method is that a large amount of information can be derived for each ELG candidate from the survey data themselves. This reduces the need for follow-up observations. The imaging data provide accurate B and V photometry, astrometry, and morphological data, while the digital objective-prism spectra allow us to measure the position and strength of the observed emission line. Of course, the objective-prism spectra are of such low resolution and small spectral range that one cannot use them to classify the ELGs by activity type (e.g., Seyfert vs. starburst). Therefore, follow-up spectra are still necessary in order to develop a more complete understanding of the nature of each ELG. Nonetheless, one can learn a great deal about the make-up of the KISS ELG sample by examining the properties of the survey constituents using the survey data alone. In the following section, we examine key characteristics of the sample, and compare the properties of the KISSB galaxies with those from previous objective-prism surveys.

4.1.1. *Magnitude & Color Distributions*

Figure 3a displays the B-band apparent magnitude distribution for the KISSB galaxies, while Figure 3b plots the B−V color distribution. The median values of both B and B−V for the KISS galaxies are indicated, as is the magnitude corresponding to the completeness limit of the Markarian survey (Mazzarella & Balzano 1986), for comparison. Clearly, the KISS sample probes substantially deeper (by ∼3 magnitudes) than the Markarian survey. The survey appears to have good sensitivity down to B = 20, beyond which it quickly drops. KISS is probably not as sensitive to bright galaxies (B < 15), because the contrast between the continuum and emission line is not sufficient to allow us to detect low equivalent width emission. We can estimate the incompleteness at these bright magnitudes in the following way. Previous studies of [O III]-selected ELG samples indicate that approximately 6.7% of the *field-galaxy* population have strong enough [O III] emission lines to be detected in a survey like KISSB (Salzer *et al.* 1989). In the area surveyed, there are only 58 CGCG galaxies (Zwicky *et al.* 1961) with B < 15, and of these 9 are located in the Coma cluster. Hence, we predict that there should be 3.3 [O III]-selected objects in our survey area with B < 15, while the actual number found is 2. Therefore, while we suspect that we are somewhat less complete at brighter magnitudes, there is no evidence that KISS is significantly incomplete here. Certainly KISSB will become progressively less sensitive to modest equivalent-width emission lines at brighter magnitudes.

In order to place the magnitude and color distributions for KISSB into better perspective, we display in Figures 4 and 5 histograms comparing the KISS galaxies to those from other surveys. Figure 4 plots histograms showing the

distributions of apparent magnitude for KISSB, the first red (Hα-selected) KISS catalog (see KR1), the Markarian survey (Mazzarella & Balzano 1986), the UM survey (Salzer *et al.* 1989), the Case survey (Salzer *et al.* 1995), and the UCM survey (Pérez-González *et al.* 2000). The median B magnitudes are indicated for each data set. Interestingly, the median depth of KISSB and KISSR are essentially identical: B = 18.17 for the blue survey and B = 18.07 for the red. This is true even though the two surveys are derived from completely independent spectral data. Despite their similar depths, the red survey detects nearly ten times more ELGs per unit area than does KISSB, a testament to the ubiquity of Hα emission. Of the samples plotted, KISSB compares most closely to the UM survey in terms of object detection method: both are primarily [O III]-selected. KISSB is roughly 1.3 magnitudes deeper than the UM survey. Similarly, KISSR and the UCM survey are both Hα-selected, with KISSR having a median brightness a full 2 magnitudes fainter.

Figure 5 shows a similar comparison, but for B−V color. In this case, only the KISSR, UM, and Markarian samples have reasonably complete BV photometry to allow for this comparison. Here the B−V colors for the Markarian galaxies are taken from Huchra (1977). Since the KISSB and UM samples have similar selection methods, it is perhaps no surprise that they have similar color distributions. The UV-excess-selected Markarian sample also exhibits a similar range and median color. In contrast, the difference between the blue and red KISS samples is substantial. The median colors, B−V = 0.50 for KISSB and B−V = 0.67 for KISSR clearly indicate that the different selection methods result in the detection of a different sample of galaxies. KISSB is biased toward detecting galaxies with large [O III] line strengths. Such galaxies tend to be either dwarfish star-forming galaxies, Seyfert galaxies with strong high-excitation spectra, or starburst galaxies with low amounts of external extinction. Hence, blue colors tend to be favored. The median B−V color is comparable to the mean color for irregular galaxies (Roberts & Haynes 1994). On the other hand, the Hα-selected red survey is able to detect *both* the intrinsically blue and/or low reddening galaxies, as well as objects such as starburst nucleus galaxies and LINERs which may have appreciable Hα but weak [O III]. That is, the red survey appears to detect the vast majority of the galaxies found by the blue survey in the areas were they overlap (see Paper I), and in addition finds a large population of galaxies that are completely missed in surveys carried out in the blue. Surveying for galaxies using the Hα selection method leads to a larger sample of ELGs with a different mix of active and star-forming galaxies than found in the [O III]-selected KISSB survey.

4.1.2. *Line Strength Distributions*

As mentioned above, the digital nature of the survey data allows us to obtain estimates of the emission-line strengths directly from the spectral images. This is extremely important, as it allows us to quantify the selection function and completeness limit for the survey directly from the survey data. Since KISS is a line-selected survey, the depth of the sample is defined in terms of the emission-line strengths, not the apparent magnitudes of the galaxies (Salzer 1989). With previous line-selected objective-prism surveys these issues could only be explored using follow-up spectra. Our method for determining the completeness of the KISS survey is detailed in Gronwall *et al.* 2002a. In this section we illustrate the distribution of equivalent widths and line fluxes from the blue survey data.

Figure 6 plots the distribution of [O III] equivalent widths for the 223 KISSB galaxies. Given the coarse nature of the objective-prism spectra, both the equivalent width (EW) and line flux measurements carry with them a fairly high uncertainty (see KR1 for a complete discussion). Despite this caveat, Figure 6 is a useful representation of the nature of the KISS ELGs. The median EW is 54 Å, somewhat higher than the median for the red survey (41 Å). The distribution of EWs is seen to rise to a peak at 30–40 Å, and to contain a large number of galaxies with EW < 30 Å. This suggests that KISS is fairly complete for objects with equivalent widths greater than ∼30 to 40 Å, but it becomes progressively more incomplete at lower values. About 13.5% of the sample have EWs > 250 Å, compared to only 3.5% for the KISSR sample.

The method used to calibrate the objective-prism fluxes is described in KR1. In brief, follow-up spectra of non-extended emission-line galaxies taken under photometric conditions are used to scale the line fluxes measured from the objective-prism spectra. The resulting line fluxes for the blue survey ELGs are illustrated in Figure 7. The median flux of 1.12×10^{-14} erg/s/cm^2 is about 30% larger than the median Hα+[N II] flux for the KISSR sample. The faintest objects detected have [O III] fluxes of $\sim 10^{-15}$ erg/s/cm^2.

4.1.3. *Redshift Distributions*

Another quantity derived from the objective-prism spectra is the redshift of each galaxy. The details of the wavelength calibration method for the spectral data are given in Paper I and Herrero *et al.* (2002). As a check of the accuracy of the method, we plot in Figure 8 a comparison between the redshifts obtained from follow-up spectroscopy for 123 KISSB ELGs (z_{SPEC}) and the redshift estimates from the survey data (z_{KISS}). The solid line indicates $z_{KISS} = z_{SPEC}$, while the dashed line shows where objects for which the line seen in the objective-prism spectrum was Hβ rather than [O III]λ5007 would be located. One such object appears to have been found by the survey (a Seyfert 1 galaxy). There is obviously good agreement between z_{KISS} and z_{SPEC}. The RMS scatter of the KISS redshifts about the unity line provides an estimate of the redshift uncertainty associated with z_{KISS}. The value σ_z = 0.0049 is obtained if the single Hβ-selected object is excluded, but the several outlying galaxies above the unity line are retained. This corresponds to a velocity uncertainty of 1470 km s^{-1}. Inspection of the finder charts for the outliers shows that they are all large galaxies with significant extension in the north-south direction (the direction of the dispersion in the objective-prism spectra). In all cases, the larger than typical redshift offset is most likely due to this extension, which can displace the location of the observed emission line relative to the center of the galaxy. If these extended outliers in Figure 8 are removed, the value of σ_z decreases to 0.0033 (989 km s^{-1}), which compares favorably to the value of σ_z = 0.0028 found for

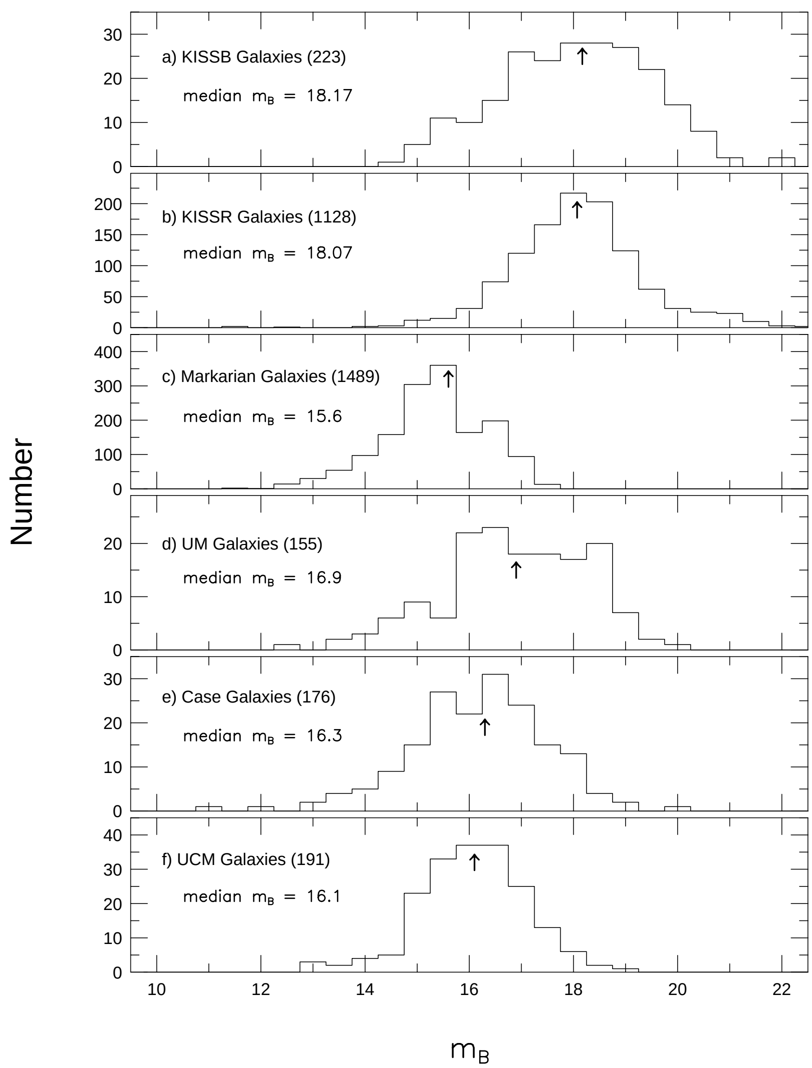

FIG. 4.— Comparison of the B-band apparent magnitude distributions for several samples of active galaxies: (a) the KISSB sample from the current paper; (b) the KISSR Hα sample from Salzer *et al.* (2001); (c) the full Markarian sample, taken from Mazzarella & Balzano (1986); (d) the [O III]-selected UM survey galaxies (Salzer *et al.* 1989); (e) the Case Survey galaxies (Salzer *et al.* 1995); (f) the Hα-selected UCM sample (Pérez-González *et al.* 2000). The number of galaxies in each sample is indicated in parentheses next to the survey name. The median apparent magnitude is indicated for each sample, and is marked by the arrow in each histogram.

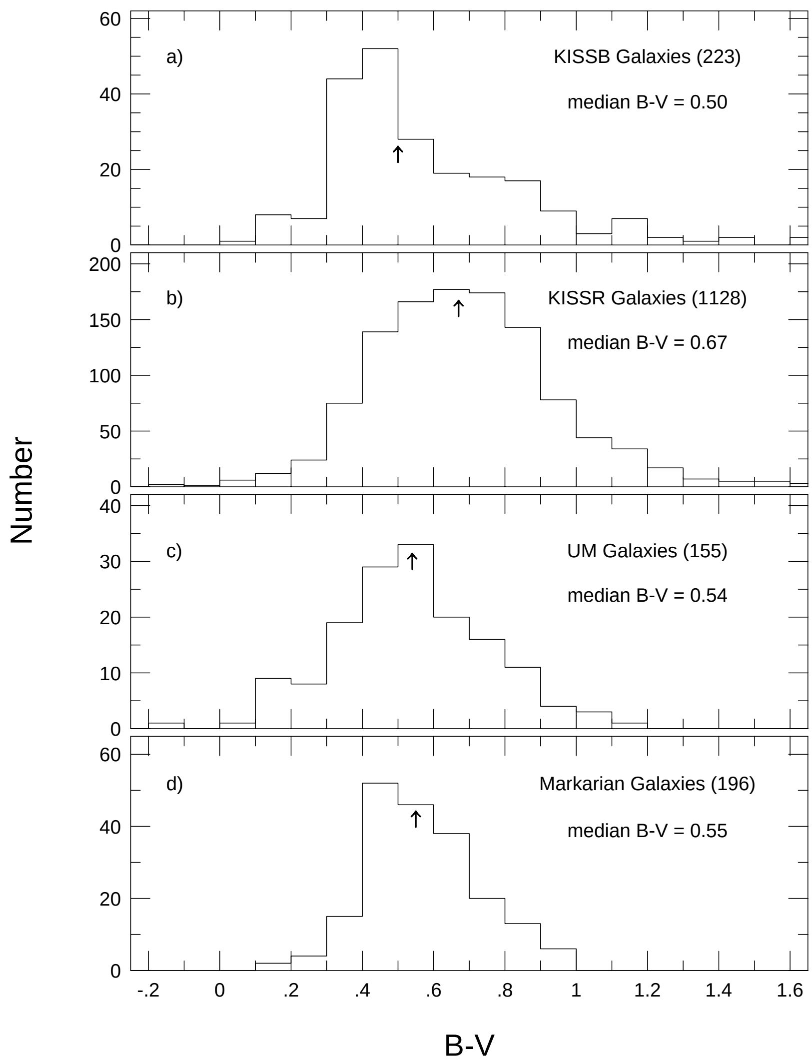

Fig. 5.— Comparison of the B−V color distributions for (a) the KISSB sample from the current paper; (b) the KISSR Hα sample from Salzer *et al.* (2001); (c) the [O III]-selected UM survey galaxies (Salzer *et al.* 1989); (d) a large sample of Markarian galaxies with UBV photometry in Huchra (1977). The median color is indicated for each sample.

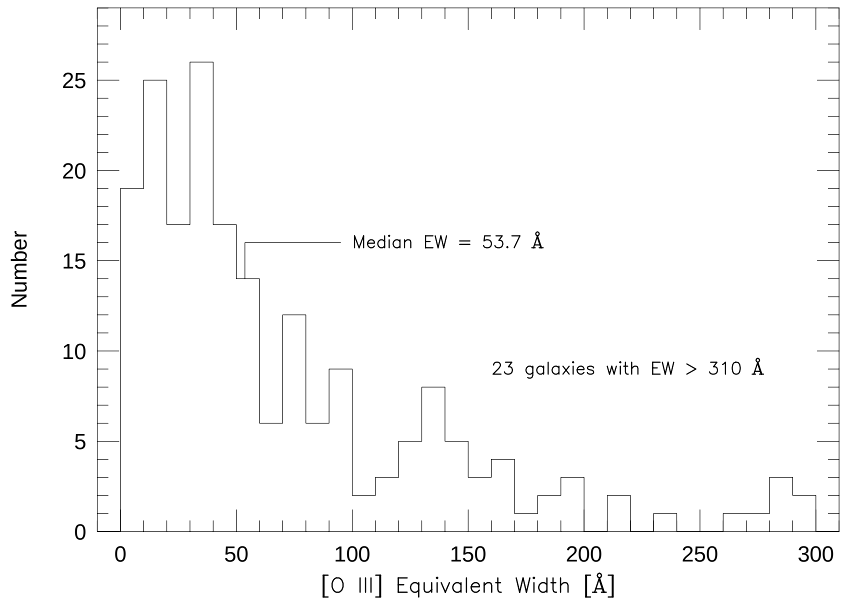

Fig. 6.— Distribution of measured [O III] equivalent widths for the KISS ELGs. The median value of 53.7 Å is indicated. The measurement of equivalent widths from objective-prism spectra tends to yield underestimates of the true equivalent widths, so these values should only be taken as estimates. The survey appears to detect most sources with EW([O III]) > 30 – 40 Å.

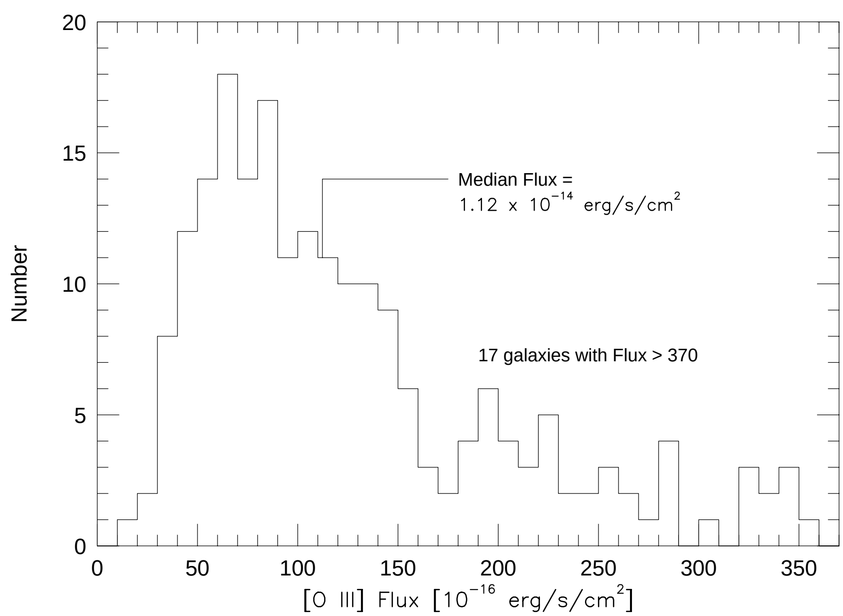

Fig. 7.— Distribution of [O III] line fluxes for the 223 KISS ELGs included in the current survey list. The median flux level is indicated.

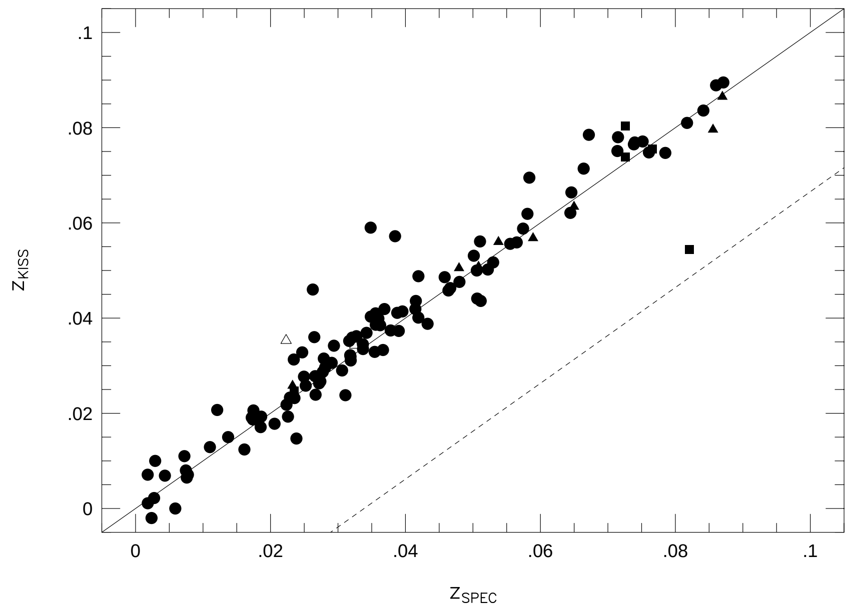

FIG. 8.— Comparison between the redshift values estimated from the objective-prism spectra (z_{KISS}) and those obtained from slit spectra (z_{SPEC}) for 123 KISSB galaxies with follow-up spectra. Symbols indicate the activity type of each galaxy: starbursting galaxies are solid circles, Seyfert 1's are solid squares, Seyfert 2's are solid triangles, and LINERs are open triangles. The solid line indicates $z_{KISS} = z_{SPEC}$, while the dashed line shows the expected location of objects for which the line detected in the objective-prism spectrum is Hβ rather than [O III]λ5007. A single Seyfert 1 galaxy appears to have been Hβ-selected.

the KISSR galaxies which have follow-up spectra (Paper I). While this level of precision is not adequate for making detailed maps of the galaxian spatial distribution, it is sufficient for mapping the coarse structures and for luminosity function work.

A similar comparison between z_{KISS} and z_{SPEC} for the red KISS sample revealed a systematic offset in the value of z_{KISS} for redshifts above about 0.07 (Paper I). It was concluded that this offset is caused by the fact that the emission line starts to redshift out of the filter bandpass used for the spectral data, and that at higher and higher redshifts more and more of the red side of the line is missing. This causes the line center measured in the objective-prism spectra to be biased to the blue of the true line center. No corresponding effect is seen in Figure 8, although the limited number of follow-up spectra, particularly above z = 0.07, make it difficult to assess whether or not a correction for this effect is necessary. Since the blue objective-prism spectra were obtained at somewhat higher dispersion than the red, it is possible that the onset of the velocity shift observed in the red survey may be reduced in significance in KISSB.

Figure 9 illustrates the redshift distributions for (a) the KISSB galaxies, and (b) the CGCG (Zwicky *et al.* 1961) galaxies located in the same area of the sky. As described in KR1, this CGCG sample was chosen as a comparison sample of "normal" galaxies in the same volume of space covered by the ELG survey. To provide adequate numbers, a 3°-wide declination strip of the CGCG is used, compared to the 1°-wide KISS strip. Redshifts for the CGCG sample come from Falco *et al.* (1999), and the sample is complete for all CGCG galaxies to B = 15.5. This comparison sample of "normal" galaxies is also used in the following section.

The median redshifts for the two samples are indicated in the figure. The KISS ELGs extend out to much greater distances than do the magnitude-limited CGCG sample. In fact, almost no CGCG galaxies are located at redshifts beyond the median of the KISSB sample. The numbers of ELGs remain fairly constant out to z = 0.09, at which point the survey filter cuts out any higher redshift objects. The modest peak at z = 0.03 in the KISS redshift distribution corresponds roughly to the location of the "Great Wall" seen in the *Slice of the Universe* (de Lapparent *et al.* 1986).

4.2. *Derived Properties*

4.2.1. *Luminosity Distribution*

We compare the luminosities of the KISSB ELGs with those of the CGCG galaxies located in the same area of the sky in Figure 10. Absolute magnitudes are computed using the redshifts and apparent magnitudes listed in Table 2 and assuming a value for the Hubble Constant of H_o = 75 km/s/Mpc. Corrections for Galactic absorption (A_B) have been applied by averaging the values for all UGC galaxies in each survey field from the compilation of Burstein & Heiles (1984). Since the majority of the survey strip is at high Galactic latitude, this correction is typically small: 65 of the 102 fields (64%) have $A_B <$ 0.05, and 92 of 102 (90%) have $A_B < 0.10$. The maximum correction of $A_B = 0.26$ occurs in the easternmost survey field (F1655). The median blue absolute magnitude of the KISS ELGs is −18.04, which is roughly two magnitudes fainter than M*, the "characteristic luminosity" parameter of the Schechter (1976) luminosity function. As seen in the lower portion of the figure, the majority of the CGCG

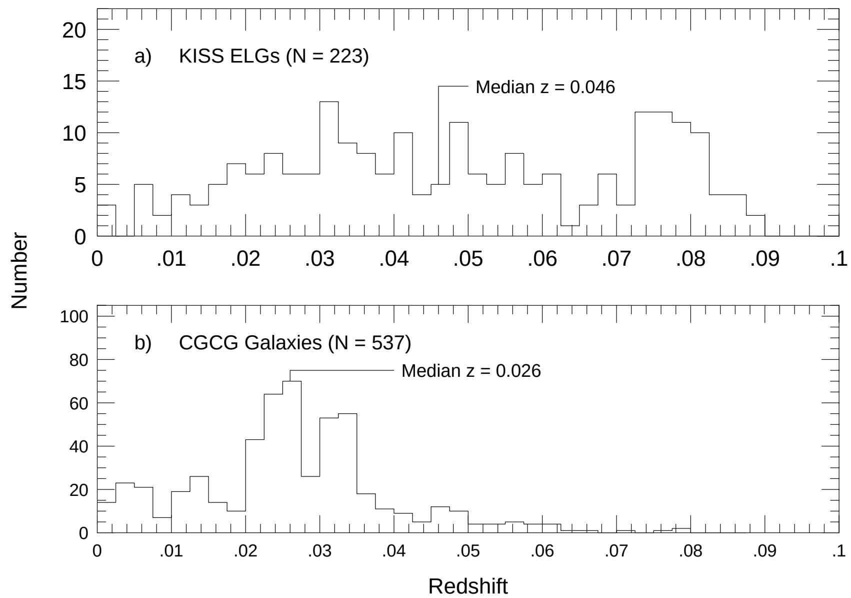

FIG. 9.— Histograms showing the distribution of redshift for (a) the 223 [O III]-selected KISS ELGs and (b) the 537 "normal" galaxies from the CGCG which are located in the same area of the sky. The median redshift is indicated in both plots. Note that the number of KISS ELGs remains fairly constant out to the cut-off of the filter used for the survey.

galaxies are more luminous than the KISS ELGs. The median absolute magnitude for the comparison sample is −20.08, which is roughly the value of M*.

In Figure 11 we present a comparison of the luminosity distributions for several other ELG samples. Included are the absolute magnitude histograms of the KISSB (this paper), KISSR (KR1), Markarian (Mazzarella & Balzano 1986), UM (Salzer 1989), and Case (Salzer *et al.* 1995) surveys. The median luminosities are labeled. The sample most similar to the KISSB survey are the UM ELGs. The two have nearly identical median values, and similarly shaped distributions. This should come as no surprise, since the two surveys employ the same primary selection method. The Hα-selected KISSR sample has a median luminosity nearly a full magnitude brighter than KISSB, while the UV-excess selected Markarian survey has a luminosity distribution more nearly similar to the magnitude-limited CGCG sample plotted in Figure 10b. The Case survey sample is intermediate between the KISSB and KISSR distributions.

Figure 11 illustrates nicely how important the selection method can be in defining the make-up of any galaxy sample. Despite the fact that KISSR and KISSB are selected using very similar methods, they contain a substantially different mix of galaxies. The only difference is whether [O III] or Hα is the emission line used in the selection of the sample, yet the make-up of the catalog changes a great deal. Even greater differences exist between magnitude-limited samples (the CGCG) and line-selected samples. Clearly, the latter are more dwarf dominated than are magnitude-limited samples. As stressed in Salzer (1989) and Lee *et al.* (2000), line-selected surveys like UM and KISS are excellent for providing large samples of dwarf galaxies at distances well beyond the Local Supercluster.

4.2.2. *Spatial Distribution*

It is also relevant to examine the spatial distribution of the KISSB galaxies, and to compare their clustering properties with respect to the CGCG galaxies. However, due to the coarse nature of the KISS objective-prism redshifts, we limit ourselves at this time to a simple visual inspection of the spatial distribution of the KISS ELGs. A more comprehensive study will have to wait until higher quality redshifts have been obtained for the full sample.

Figure 12a shows the spatial distribution of the KISSB galaxies out to a redshift of 15,000 km s^{-1}, where the velocities plotted are based on the redshifts listed in Table 2. The ELGs are plotted as the larger open circles. The CGCG galaxy sample, described in the previous section, is plotted for comparison as smaller dots. As was seen previously in KR1, which covers the R.A. range from 12^h 15^m to 17^h 0^m (i.e., the upper 56% of the figure), the ELGs tend to lie along the large-scale structures defined by the CGCG galaxies, but with a tendency toward being somewhat less clustered. This behavior has been seen before in several other samples of ELGs (e.g., Salzer 1989, Rosenberg *et al.* 1994, Pustil'nik *et al.* 1995, Popescu *et al.* 1997, Lee *et al.* 2000). A number of KISSB galaxies appear to be located in voids. However, **given the low level of precision in the objective-prism redshifts, the locations of these objects should be considered tentative until confirming follow-up spectra can be obtained**. Once these spectra exist, we plan to carry out a detailed analysis of the clustering characteristics of the KISS sample.

The two samples are plotted again in Figure 12b, this time out to a redshift limit of 30,000 km s^{-1}. The CGCG sample has few galaxies with redshifts beyond 15,000 km s^{-1}, so there is little room for comparisons in this figure. We note that the KISSB galaxies populate the re-

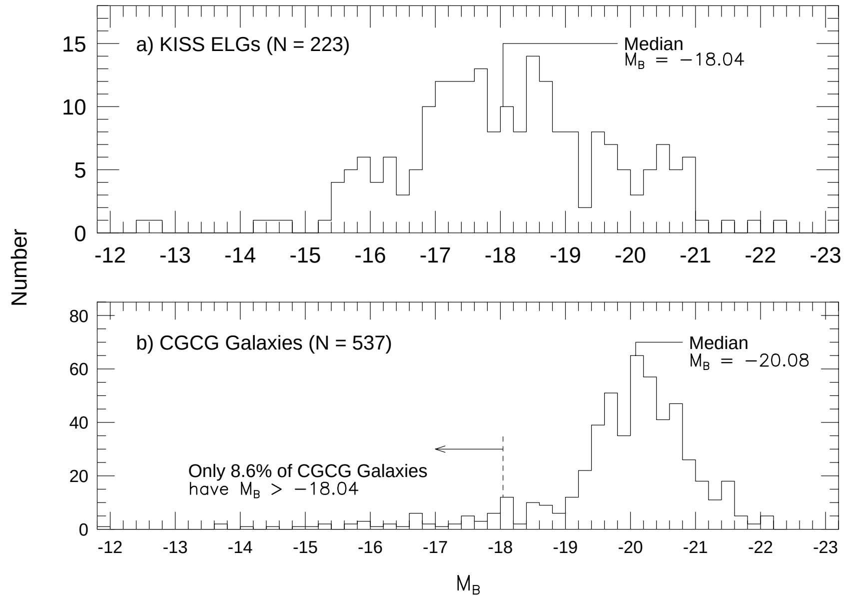

FIG. 10.— Histograms showing the distribution of blue absolute magnitudes for (a) the 223 [O III]-selected KISS ELGs and (b) the 537 "normal" galaxies from the CGCG that are located in the same area of the sky. The median luminosity of each sample is indicated. The KISS ELG sample is made up of predominantly intermediate- and lower-luminosity galaxies, making this line-selected sample particularly powerful for studying dwarf galaxies.

gion out to ~25,000 km s^{-1} fairly uniformly, beyond which point the numbers drop suddenly. This effect is due to the filter used for the objective-prism observations, which cuts off the sample quite abruptly between redshifts of 0.08 and 0.09 (see Figure 9). Although the CGCG galaxies do not extend out to the higher redshift range plotted here, the Century Redshift Survey (CRS, Geller *et al.* 1997; Wegner *et al.* 2001) sample does. Comparison with Figure 1 of Geller *et al.* suggests that the higher redshift KISSB galaxies also tend to fall along filaments defined by the CRS galaxies, and that the low density region located at ~18,000 km s^{-1} in the lower half of the diagram is also present in the CRS data.

A more complete analysis of the spatial distribution and clustering properties of the KISSB ELGs will be carried out once follow-up spectra for a larger fraction of them are available. Important issues that can be addressed include the environments of AGN and starburst galaxies as well as the nature of ELGs located in voids.

4.3. *Comparison with Previous Surveys*

The KISS project builds upon the successes of previous objective-prism surveys, some of which have searched for objects in the same area of the sky. It is useful, therefore, to compare the degree to which KISS overlaps with these previous surveys. It is important to keep in mind the different selection methods of the various surveys in making such a comparison. For example, it was found in KR1 that KISS showed excellent overlap with the previous line-selected surveys that searched the same parts of the sky (Wasilewski 1983; UCM: Zamorano *et al.* 1994), but had a lower level of agreement with color or UV-excess selected samples (Markarian 1967; Case: Pesch & Sanduleak 1983).

As was already mentioned, there are 125 KISSB objects in the area covered by KR1. Of these, 113 (90%) are cataloged as KISSR or KISSRx objects in KR1. Since there are 1128 KISSR galaxies and 189 KISSRx objects in this area, less than 10% of the Hα-selected objects are recovered in the [O III]-selected sample. This is an important point! The two samples reach to the same emission-line flux levels, the same apparent magnitudes, and cover the same volumes (due to the survey filters). Yet the Hα-selection process yields ~10 times more objects per unit area than does the [O III]-selection method. Clearly, strong Hα emission is more ubiquitous than strong [O III] emission. Many galaxies which exhibit significant activity may have weak lines in the blue portion of the spectrum (e.g., LINERS, highly reddened starbursts or Seyfert 2s). For this reason, we have chosen to continue the KISS project working exclusively in the red portion of the spectrum for all future ELG catalogs.

Given the results obtained from comparing KISSB to KISSR, it is not surprising that KISSB fails to recover a number of objects cataloged in other previous surveys as well. Most of this can be understood as being due to different selection methods. There are 15 Markarian galaxies and 114 Case galaxies in the area covered by the current survey. Only four Markarian galaxies and 35 Case galaxies are cataloged in KISSB (27% and 31%, respectively). Since the Markarian survey is a UV-excess survey and Case is primarily color selected (Salzer *et al.* 1995), the low percentages of overlap with these surveys is no great surprise. KISSB fares slightly better with the line-selected UCM (11 of 23, 48%) and Wasilewski (9 of 11, 82%) surveys. Since UCM is Hα selected, one should not expect perfect overlap with KISSB (even though KISSR recovers 100% of the UCM galaxies in the areas where the two surveys over-

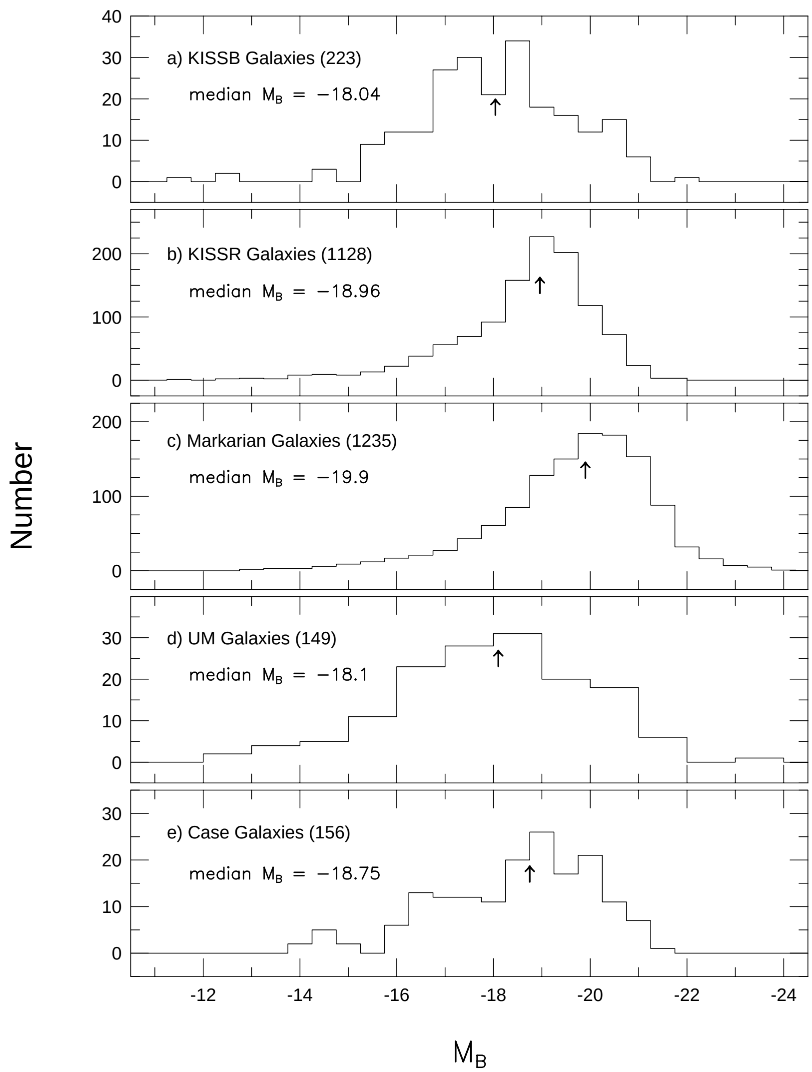

FIG. 11.— Comparison of the B-band absolute magnitude distributions for several samples of galaxies: (a) the KISSB sample from the current paper; (b) the KISSR Hα sample from Salzer *et al.* (2001); (c) the full Markarian sample, taken from Mazzarella & Balzano (1986); (d) the [O III]-selected UM survey galaxies (Salzer *et al.* 1989); (e) the Case Survey galaxies (Salzer *et al.* 1995). The median value for each survey is indicated. The KISSB and UM samples are quite comparable, both in terms of the shapes of the distributions and the median values. The differences between the various surveys can be understood in terms of their selection methods (see text).

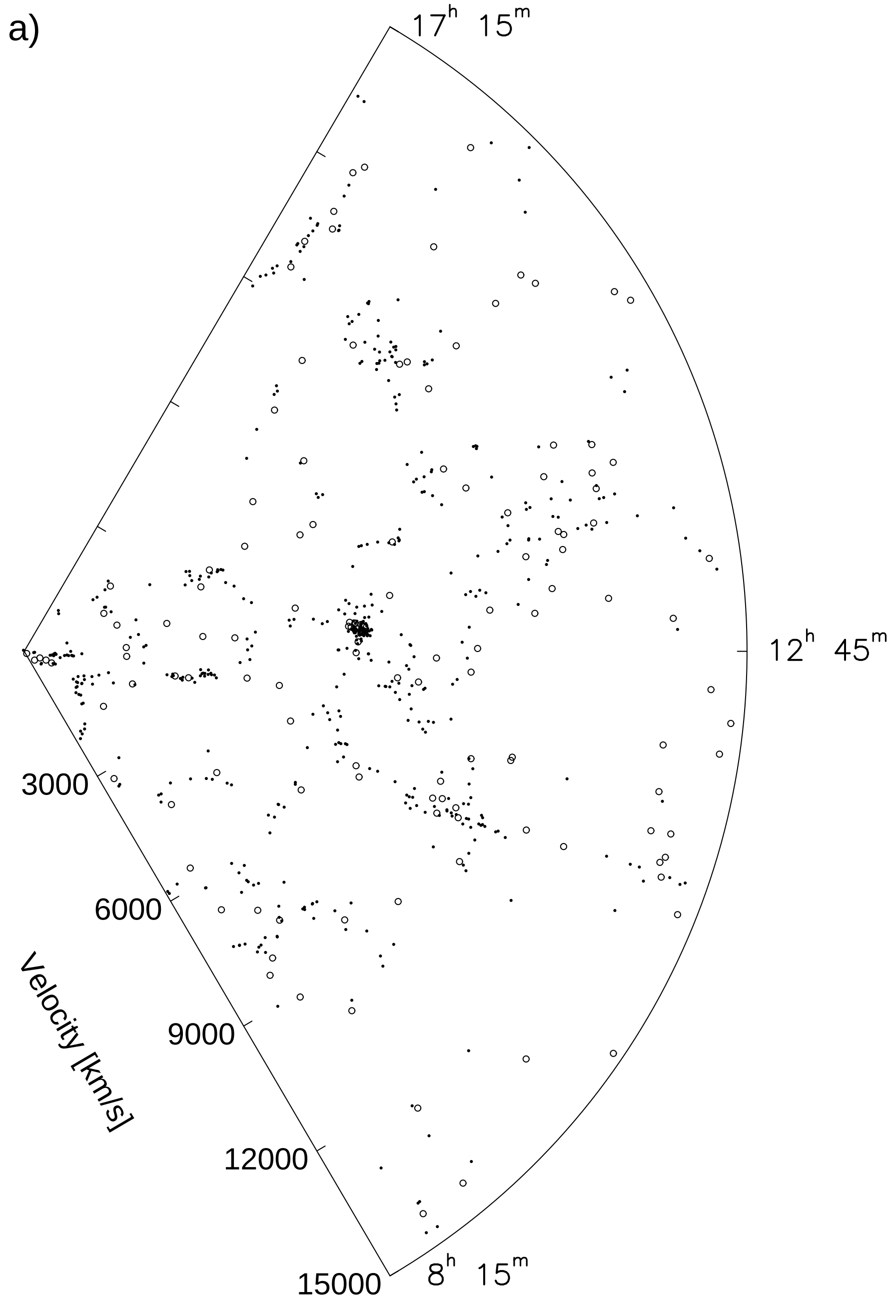

FIG. 12.— The spatial distribution of the KISS ELGs. The CGCG comparison sample is displayed as small dots, while the ELGs are larger, open symbols. (a) Velocities plotted out to 15,000 km s^{-1}. The ELGs are seen to trace the large-scale structures defined by the CGCG galaxies at low redshift. However, they exhibit the appearance of being less tightly clustered. A large number of ELGs are located in voids. (b) Velocities plotted out to 30,000 km s^{-1}. At larger distances the ELGs appear to reveal several structures not visible in the shallower CfA2 redshift catalog. The numbers of ELGs remains high out to ∼25,000 km s^{-1}.

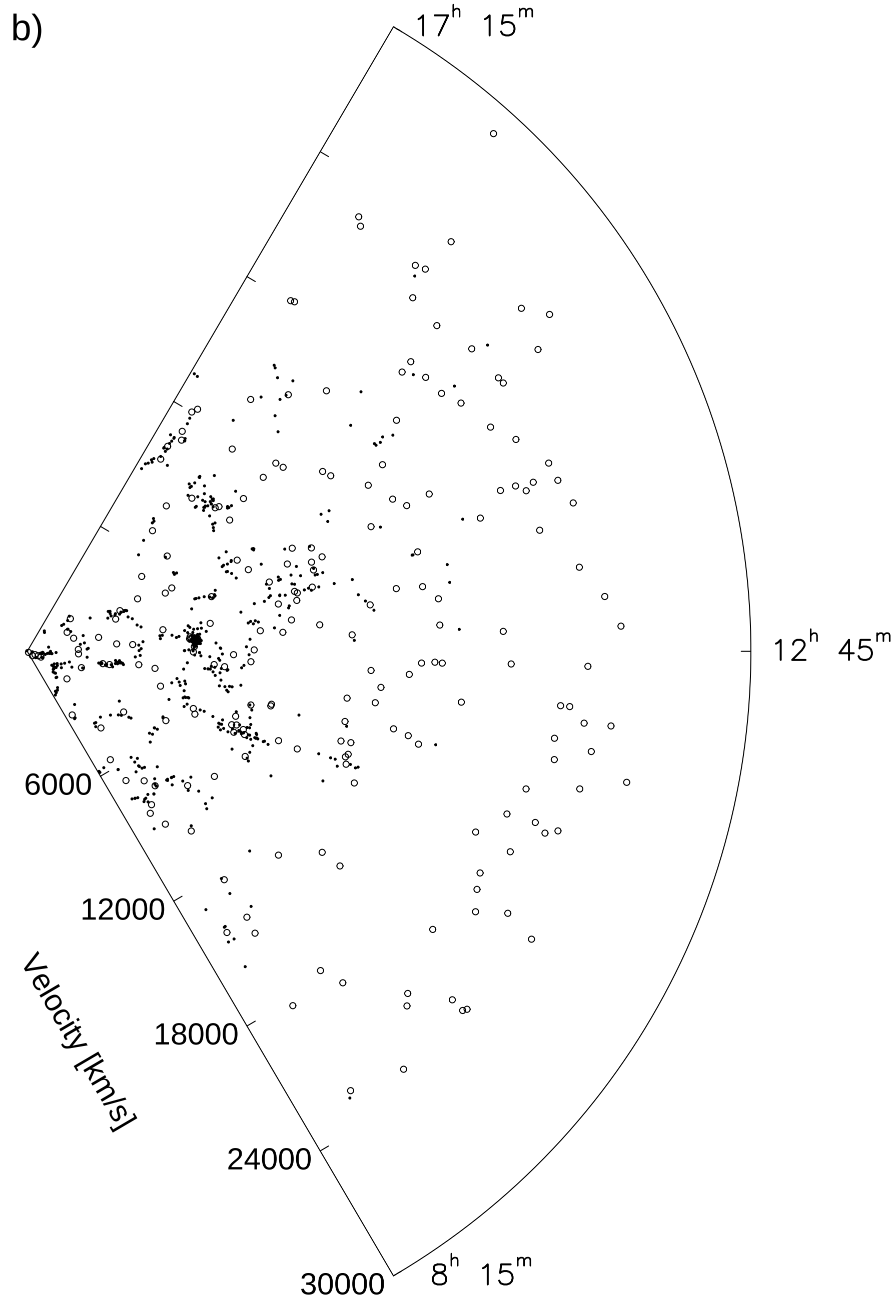
b)
17h 15m
12h 45m
8h 15m
6000
12000
18000
24000
30000
Velocity [km/s]

lap). However, the Wasilewski survey is [O III] selected, like KISSB, and also has a much brighter limiting magnitude. Hence, one might have expected a higher degree of overlap. We examined objective-prism data for the two Wasilewski objects not recovered (Was 12 and Was 88), and found that both are bright galaxies with no hint of emission in our spectra. It seems likely that both possess, at best, weak emission lines. Was 12 is described as a blue elliptical galaxy in Wasilewski (1983), while Was 88 is listed as having only weak [O III] emission by Bothun *et al.* (1989).

5. SUMMARY

We present our second list of emission-line galaxies discovered as part of the KPNO International Spectroscopic Survey (KISS). This is the first list of [O III]-selected ELGs. A total of 223 galaxies are included in this survey list, which covers an area of 116.6 deg^2. With a surface density of 1.91 ELGs per deg^2, the blue portion of KISS finds more than 19 times the number of AGNs and starbursting galaxies per unit area than the Markarian survey, and nearly 4 times the number found by the UM survey, which used a similar selection method. An additional 91 ELG candidates detected with a slightly lower level of statistical significance are cataloged in a supplementary list (see appendix). The main advantages of KISS over previous photographic surveys are the combination of increased depth and wavelength coverage afforded by the use of a CCD as the survey detector.

The digital nature of the survey data, which includes both imaging and spectral observations, means that a great deal of information is available for each object in the sample. In addition to tabulating the ELG candidates, Table 2 also includes accurate astrometry, B and V photometry, estimates of the redshift, and emission-line strength information for all objects in the catalog. This allows us to investigate the properties of the survey constituents without the need for detailed follow-up observations. We illustrate the distributions of apparent magnitudes, colors, emission-line strengths, redshifts, and absolute magnitudes for the full sample of KISSB ELGs. The new catalog of ELGs is found to have an apparent magnitude distribution very similar to that of KISSR, with a median B magnitude of 18.17. Not surprisingly, the typical colors of the KISSB galaxies are somewhat bluer than those for KISSR. Based on the distribution of measured emission-line equivalent widths, we estimate that KISSB detects most ELGs in the survey area with [O III] EW > 30 Å. The luminosity distribution is skewed toward lower luminosities (median $M_B = -18.04$) than KISSR. This last item is an interesting result, and is due to the use of [O III]λ5007 rather than Hα as the primary emission line used to select the survey constituents. While KISSR and KISSB are in all other aspects similar surveys, selecting the ELGs via the two different emission lines changes the make-up of the respective samples in a major way.

We also compare the properties of the KISS galaxies with those of previous surveys (e.g., Markarian, Case, UM, UCM) in order to evaluate the relative strengths of each, as well as to better understand how their selection functions help to shape the nature of the resulting samples. The KISSB galaxies are fainter (by 1.3 to 2.6 magnitudes on average) than the galaxies detected in this representative sample of photographic surveys. The physical characteristics of the KISSB ELGS (e.g., color and luminosity) compare most closely with those of the UM survey, which is also [O III] selected. Like the UM survey ELGs, the KISSB galaxies possess a wide range to physical properties and activity levels, and include both luminous starbursting and Seyfert galaxies, as well as many intermediate- and low-luminosity star-forming systems.

We note that, despite the wealth of information available for the KISS ELGs from the survey data alone, follow-up spectra are still required in order to confirm each source as a *bona fide* emission-line galaxy. In addition, these spectra are necessary for providing more accurate redshifts as well as emission-line strengths in order to classify each ELG by their activity type (i.e., AGN *vs.* starburst). To date, we have obtained follow-up spectra for slightly more than half of the KISSB candidates; 119 of 123 KISSB candidates with spectra are found to be real ELGS (97%). Additional follow-up spectroscopic observations are in progress for large subsets of the KISS ELG catalogs.

Additional lists of ELG candidates are currently being prepared for publication (e.g., Gronwall *et al.* 2002b), and observational data continue to be obtained for new survey areas. All future observations will focus on the Hα portion of the spectrum, for the reasons described in the text. The overall goals of the KISS survey are to cover roughly 300 sq. deg. of sky, and to catalog in excess of 5000 ELG candidates.

We gratefully acknowledge financial support for the KISS project from an NSF Presidential Faculty Award to JJS (NSF-AST-9553020), which was instrumental in allowing for the international collaboration. Additional support for this project came from NSF grant AST-9616863 to TXT, and from Kitt Peak National Observatory, which purchased the special filters used by KISS. Summer research students Michael Santos, Laura Brenneman, and Erin Condy, supported by the Keck Northeast Astronomy Consortium student exchange program, helped to reduce the survey data presented in the current paper. We are grateful to Laura Chomiuk, who assisted in the final production of this paper, and to Katherine Rhode and Anna Jangren for their critical reading of the manuscript. Several useful suggestions by the anonymous referee helped to improve the presentation of this paper. We thank the numerous colleagues with whom we have discussed the KISS project over the past several years, including Jesús Gallego, Rafael Guzmán, Rob Kennicutt, and David Koo. Finally, we wish to thank the support staff of Kitt Peak National Observatory for maintaining the Burrell Schmidt telescope and instrument during the early years of the project, and the Astronomy Department of Case Western Reserve University for taking over this role after 1997.

APPENDIX

SUPPLEMENTARY TABLE OF 4σ OBJECTS

As explained in Section 3, the main selection criterion used to decide whether or not an object is included in the KISS catalog is the presence of a 5σ emission feature in its spectrum. Because of the high sensitivity of the survey data, many objects were detected with emission lines that were slightly weaker than this level. We made the decision to exclude such objects from the main survey lists, in order to preserve the statistically complete nature of the sample. It was felt that the high degree of reliability of the sample would be compromised somewhat if these objects were included. However, rather than ignore these weaker-lined ELG candidates entirely, we are publishing them in a supplementary table.

Listed in Table 3 are 91 ELG candidates that have emission lines detected at between the 4σ and 5σ level. The format of Table 3 is the same as for Table 2, except that the objects are now labeled with KISSBx numbers ('x' for extra). The full version of the table, as well as finder charts for all 91 KISSBx galaxies, are available in the electronic version of the paper.

The characteristics of the supplementary ELG sample are similar to those of the main survey ELGs, although with some predictable differences. The median [O III] equivalent width is 30.3 Å, substantially below the value for the main sample. The KISSBx galaxies are somewhat fainter (median B magnitude of 18.76) and significantly redder (median B−V = 0.90). Their median redshift is significantly higher than that of the main sample (0.069), while their median luminosity is slightly higher (−18.3). Hence, the supplementary ELG list appears to be dominated by intermediate luminosity galaxies with a somewhat lower rate of star-formation activity (lower equivalent widths, redder colors) than the ELGs in the main sample.

REFERENCES

Bothun, G. D., Halpern, J. P., Lonsdale, C. J., Impey, C., & Schmitz, M. 1989, ApJS, 70, 271
Burstein, D., & Heiles, C. 1984, ApJS, 54, 33
de Lapparent, V., Geller, M. J., & Huchra, J. P. 1986, ApJ, 302, L1
Falco, E. E., Kurtz, M. J., Geller, M. J., Huchra, J. P., Peters, J., Berlind, P., Mink, D. J., Tokarz, S. P., & Elwell, B. 1999, PASP, 111, 438
Geller, M. J., Kurtz, M. J., Wegner, G., Thorstensen, J. R., Fabricant, D. G., Marzke, R. O., Huchra, J. P., Schild, R. E., & Falco, E. E. 1997, AJ, 114, 2205
Gronwall, C., Salzer, J. J., Brenneman, L., Condy, E., & Santos, M. 2002a, in preparation
Gronwall, C., Salzer, J. J., Sarajedini, V. L., Chomiuk, L. B., Moody, J. W., Frattare, L. M., & Boroson, T. A. 2002b, in preparation
Herrero, J. L., Frattare, L. M., Salzer, J. J., Gronwall, C., & Kearns, K. 2002, PASP, submitted
Huchra, J. P. 1977, ApJS, 35, 171
Lee, J. C., Salzer, J. J., Law, D. A., & Rosenberg, J. L. 2000, ApJ, 536, 606
Lipovetsky, V., Engels, D., Ugryumov, A., Hopp, U., Richter, G., Izotov, Y., Kniazev, A., & Popescu, C. 1998, in *I.A.U. Symposium No. 179: New Horizons from Wide-Field Imaging*, eds. B. J. McLean, D. A. Golombek, J. J. Hayes, and H. E. Payne. (Kluwer), p 299
MacAlpine, G. M., Smith, S. B., & Lewis, D. W. 1977, ApJS, 34, 95
Markarian, B. E. 1967, Astrofizika, 3, 55
Markarian, B. E., Lipovetskii, V. A., & Stepanian, D. A. 1983, Astrofizika, 19, 29
Mazzarella, J. M., & Balzano, V. A. 1986, ApJS, 62, 751
Nilson, P. 1973, *Uppsala General Catalogue of Galaxies*, (Uppsala: Roy. Soc. Sci. Uppsala)
Pérez-González, P. G., Zamorano, J., Gallego, J., & Gil de Pez, A. 2000, A&AS, 141, 409
Pesch, P., & Sanduleak, N. 1983, ApJS, 51, 171
Popescu, C. C., Hopp, U., & Elsässer, H. 1997, A&A, 328, 756
Popescu, C. C., Hopp, U., Hagen, H. J., & Elsässer, H. 1996, A&AS, 116, 43
Pustil'nik, S., Ugryumov, A. V., Lipovetsky, V. A., Thuan, T. X., & Guseva, N. 1995, ApJ, 443, 499
Roberts, M. S., & Haynes, M. P. 1994, ARA&A, 32, 115
Rosenberg, J. L., Salzer, J. J., & Moody, J. W. 1994, AJ, 108, 1557
Salzer, J. J. 1989, ApJ, 347, 152
Salzer, J. J., Gronwall, C., Lipovetsky, V. A., Kniazev, A., Moody, J. W., Boroson, T. A., Thuan, T. X., Izotov, Y. I., Herrero, J. L., & Frattare, L. M. 2000, AJ, 120, 80 (Paper I)
Salzer, J. J., Gronwall, C., Lipovetsky, V. A., Kniazev, A., Moody, J. W., Boroson, T. A., Thuan, T. X., Izotov, Y. I., Herrero, J. L., & Frattare, L. M. 2001, AJ, 121, 66 (KR1)
Salzer, J. J., MacAlpine, G. M., & Boroson, T. A. 1989, ApJS, 70, 479
Salzer, J. J., Moody, J. W., Rosenberg, J. L., Gregory, S. A., & Newberry, M. V. 1995, AJ, 109, 2376
Schechter, P. L. 1976, ApJ, 203, 297
Smith, M. G., Aguirre, C., & Zemelman, M. 1976, ApJS, 32, 217
Surace, C., & Comte, G. 1998, A&AS, 133, 171
Wasilewski, A. J. 1983, ApJ, 272, 68
Wegner, G., *et al.* 2001, AJ, 122, in press
Zamorano, J., Rego, M., Gallego, J., Vitores, A. G., González-Riestra, R., & Rodríguez-Caderot, G. 1994, ApJS, 95, 387
Zwicky, F., Herzog, E., Kowal, C. T., Wild, P., & Karpowicz, M. 1961–1968, *Catalogue of Galaxies and Clusters of Galaxies*, (Pasadena: CIT) (CGCG)

Table 1
KISS Blue Survey Observing Runs

Dates of Run (1)	Number of Nights[a] (2)	Number of Fields – Direct[b] (3)	Number of Fields – Spectral[b] (4)
March 19 – 23, 1994[c]	2	...	...
April 13 – 17, 1994	4	...	19
April 18 – 24, 1995	5	5	11
April 29 – May 4, 1995	5	16	13
March 12 – 18, 1996	4	10	17
May 8 – 23, 1996	15	54	32
February 12 – 15, 1997	2	12	...
April 30 – May 2, 1997	3	5	10

[a]Number of nights during run that data were obtained.

[b]Number of survey fields observed.

[c]Initial run – only test data obtained.

Table 2
List of Candidate ELGs[1]

KISSB # (1)	Field (2)	ID (3)	R.A. (J2000) (4)	Dec. (J2000) (5)	B (6)	B−V (7)	z_{KISS} (8)	Flux[a] (9)	EW [Å] (10)	Qual. (11)	KISSR (12)	Comments (13)
1	F0830	3627	8 33 23.1	29 32 18.5	15.38	0.46	0.0110	36	1	1		UGC 4469
2	F0830	1711	8 34 35.6	29 17 00.2	18.18	0.20	0.0491	86	35	2		
3	F0835	905	8 39 49.3	28 57 48.2	18.20	0.67	0.0787	80	33	1		
4	F0835	512	8 40 02.4	29 49 02.6	15.99	0.98	0.0634	345	29	1		
5	F0840	2654	8 42 45.4	29 23 59.6	16.28	0.96	0.0288	164	16	1		
6	F0840	1805	8 43 37.7	29 19 21.8	17.14	0.27	0.0230	153	44	1		
7	F0840	1557	8 43 52.3	29 26 14.6	17.62	0.56	0.0193	83	32	2		
8	F0845	1172	8 49 01.3	29 29 16.6	17.55	0.39	0.0313	418	195	1		
9	F0845	455	8 49 59.1	29 40 51.1	18.64	0.46	0.0516	208	138	2		
10	F0845	144	8 50 25.0	29 40 51.4	16.96	0.70	0.0279	79	11	1		
11	F0850	1115	8 54 05.2	29 07 55.8	19.74	0.57	0.0491	198	456	2		
12	F0855	484	9 00 08.5	28 55 24.2	19.13	0.38	0.0428	100	132	1		
13	F0900	1510	9 04 09.5	29 48 20.4	15.41	0.45	0.0246	35	2	2		
14	F0905	4473	9 05 41.3	28 56 36.5	19.14	1.26	0.0813	71	62	2		
15	F0905	3193	9 07 07.2	29 06 05.5	18.72	0.14	0.0344	69	126	2		
16	F0905	3069	9 07 08.5	29 28 49.7	16.83	0.50	0.0621	118	26	1		
17	F0910	3290	9 11 13.5	29 46 22.1	19.63	0.44	0.0656	171	510	2		
18	F0910	2022	9 13 05.0	28 48 44.4	19.54	0.56	0.0262	190	338	1		
19	F0910	1396	9 13 48.7	29 10 21.8	15.03	0.52	0.0150	280	14	1		UGC 4860, CG 11
20	F0925	2132	9 27 25.4	29 25 18.6	17.26	0.36	0.0748	221	56	1		
21	F0930	1460	9 33 37.3	28 45 32.7	19.63	1.69	0.0737	841	2870	1		
22	F0935	3726	9 36 07.6	29 06 44.7	15.32	0.52	-0.0004	336	19	1		CG 23
23	F0935	158	9 40 12.7	29 35 29.8	16.32	0.24	0.0012	143	37	1		
24	F0940	2414	9 42 40.6	28 52 00.4	17.64	0.35	0.0296	70	42	2		
25	F0940	1009	9 44 18.7	29 27 47.2	19.60	1.83	0.0793	126	72	1		
26	F0940	776	9 44 44.3	28 46 34.4	18.24	0.56	0.0816	51	24	3		
27	F0940	261	9 45 12.7	29 42 54.9	20.04	0.65	0.0460	159	464	2		
28	F0940	146	9 45 23.1	29 23 21.9	16.92	0.76	0.0820	100	19	2		
29	F1005	3849	10 06 18.1	28 56 40.8	14.64	0.52	0.0069	482	21	1		CG 50
30	F1005	3288	10 06 48.2	29 29 10.2	16.89	0.65	0.0707	59	7	2		

[1]Note.— The complete version of this table is presented in the electronic edition of the Journal. A portion is shown here for guidance regarding its content and format.

[a]Units of 10^{-16} erg/s/cm^2

TABLE 3
LIST OF 4σ CANDIDATE ELGs[1]

KISSBx #	Field	ID	R.A. (J2000)	Dec. (J2000)	B	B−V	z_{KISS}	Flux[a]	EW [Å]	Qual.	KISSR	Comments
(1)	(2)	(3)	(4)	(5)	(6)	(7)	(8)	(9)	(10)	(11)	(12)	(13)
1	F0845	1865	8 48 10.5	29 29 28.9	15.61	0.89	0.0806	29	1	2		
2	F0850	3556	8 51 18.4	29 23 59.0	17.91	0.92	0.0851	51	17	2		
3	F0850	47	8 55 18.8	29 51 09.3	19.21	1.68	0.0838	57	25	2		
4	F0855	458	9 00 10.8	28 55 41.8	19.27	0.30	0.0432	33	30	2		
5	F0900	630	9 04 58.8	29 51 36.9	17.51	0.50	0.0798	21	5	3		
6	F0910	1782	9 13 17.1	29 07 00.0	16.67	0.48	0.0782	96	20	1		
7	F0910	1363	9 13 53.2	29 04 41.0	16.71	0.77	0.0560	91	11	1		
8	F0915	2738	9 18 32.0	29 43 37.1	18.66	1.69	-0.0119	157	87	2		
9	F0935	2336	9 37 41.5	29 15 19.3	19.78	1.51	0.0296	32	51	2		
10	F0940	4063	9 40 31.8	28 58 09.8	15.83	0.46	0.0399	24	1	2		UGC 5154, CG 27
11	F0940	2256	9 42 51.7	28 59 60.0	16.80	0.32	0.0331	29	5	2		
12	F0940	279	9 45 12.3	29 39 32.6	19.34	1.08	0.0548	56	63	3		
13	F0950	2455	9 51 05.6	29 47 29.7	19.46	1.00	0.0716	78	133	2		
14	F1000	887	10 04 28.1	29 14 42.3	18.99	0.43	0.0443	93	112	2		
15	F1000	762	10 04 38.6	29 11 46.7	18.65	0.41	0.0164	93	109	2		
16	F1005	3064	10 07 00.4	29 43 17.3	19.42	1.41	0.0363	37	34	2		
17	F1005	511	10 09 45.1	29 39 32.1	19.05	1.26	0.0765	41	27	2		
18	F1010	4499	10 10 25.5	28 53 54.7	17.21	0.53	0.0417	47	8	2		
19	F1015	731	10 19 24.9	29 45 03.7	17.02	0.95	0.0499	57	10	2		
20	F1035	1675	10 38 19.5	29 26 23.8	20.78	0.90	0.0861	60	348	2		
21	F1045	3716	10 45 20.1	29 29 09.6	17.56	0.99	0.0551	20	3	3		
22	F1050	1288	10 53 37.3	29 21 34.5	19.21	1.43	0.0667	58	30	2		
23	F1055	2916	10 56 26.6	28 51 02.4	18.83	0.61	0.0712	73	96	3		
24	F1100	3477	11 02 11.2	29 06 29.6	19.20	0.76	0.0672	50	66	2		
25	F1110	3530	11 10 21.2	29 28 05.3	18.24	0.10	0.0750	45	35	2		
26	F1115	1748	11 18 05.7	29 23 54.9	18.62	0.27	0.0488	39	28	2		
27	F1120	3566	11 20 30.5	29 12 02.9	16.99	1.11	0.0282	58	9	1		
28	F1140	3025	11 40 59.6	29 13 30.3	20.08	0.49	0.0878	51	92	2		
29	F1140	1881	11 42 43.8	28 57 20.3	18.98	0.36	0.0591	59	52	2		
30	F1145	3182	11 46 01.3	29 24 52.5	19.57	1.34	0.0819	120	339	2		

[1]Note.— The complete version of this table is presented in the electronic edition of the Journal. A portion is shown here for guidance regarding its content and format.

[a]Units of 10^{-16} erg/s/cm^2